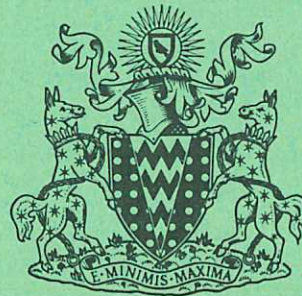


This document is intended for publication in a journal, and is made available on the understanding that extracts or references will not be published prior to publication of the original, without the consent of the author.



United Kingdom Atomic Energy Authority
RESEARCH GROUP

Preprint

EQUILIBRIUM DIFFUSION IN A TOROIDAL RESISTIVE PLASMA

T. E. STRINGER

Culham Laboratory
Abingdon Berkshire

1969

Enquiries about copyright and reproduction should be addressed to the
Librarian, UKAEA, Culham Laboratory, Abingdon, Berkshire, England

EQUILIBRIUM DIFFUSION IN A TOROIDAL RESISTIVE PLASMA

by

T.E. STRINGER

(To be submitted for publication in Physics of Fluids)

A B S T R A C T

The equilibrium equations are solved, including resistivity, parallel viscosity, and a radial electric field. A resonance effect occurs when the frequency of the electric rotation about the minor axis approaches the frequency of a natural plasma mode. For arbitrary steady electric fields the ion and electron diffusion rates are unequal, and the space charge inevitably builds up until the two rates equalise. In most conditions of interest this ambipolar electric field is close to the resonance value, and the ambipolar diffusion rate is much larger than the Pfirsch and Schlüter rate.

U.K.A.E.A. Research Group,
Culham Laboratory,
Nr. Abingdon,
Berks.

July, 1969

(MEJ)

C O N T E N T S

	<u>Page</u>
I. INTRODUCTION	1
II. THE MODEL	4
III. EQUILIBRIUM ANALYSIS	6
IV. EVALUATION OF THE DIFFUSION	10
V. THE AMBIPOLAR CONDITION	12
VI. BUILD-UP TIME FOR THE AMBIPOLAR POTENTIAL DISTRIBUTION	16
VII. A TYPICAL AMBIPOLAR POTENTIAL DISTRIBUTION	19
VIII. CONCLUSIONS	20
ACKNOWLEDGEMENT	21
REFERENCES	22
APPENDIX	23

I. INTRODUCTION

In many toroidal confinement devices the observed fluctuating fields appear to be insufficient to account for the measured diffusion across the confining field. This suggests that the diffusion is a feature of the equilibrium, rather than a result of the instabilities predicted by linear stability theory.

That finite resistivity can lead to a steady diffusion in a toroidal plasma, additional to that in a comparable straight plasma column, was first shown by Kruskal and Kulsrud¹. Assuming a simple Ohm's law, $E_{\parallel} = \eta j_{\parallel}$, they found a steady diffusion such that the decrease in compressional energy balances the Ohmic dissipation by the currents necessary to maintain equilibrium. The guiding center drift of ions and electrons in a toroidal field produces a charge separation which must be neutralised by current flow along the magnetic field. Pfirsch and Schlüter² evaluated the Ohmic dissipation by such currents in an axisymmetric torus, and obtained a diffusion rate which exceeds that for a comparable straight column by a factor $1 + 4\pi^2/\iota^2$ (where ι is the rotational transform). They also analysed in detail the azimuthal dependence of all the equilibrium variables and found a net outward flux equal to that deduced from the energy argument. Their result was rederived more concisely by Knorr³.

In all the above treatments the equilibrium density is constant over magnetic surfaces. This is a consequence of the neglect of ion inertia and viscosity. It was recently pointed out by Stringer⁴ that in the presence of a radial electric field the rotation of the plasma about its minor axis introduces an inertia term. This must be balanced by a density variation along the magnetic field lines. Such radial

electric fields are observed experimentally. The diffusion was found to be inversely proportional to the plasma dielectric constant for a frequency equal to the electric rotation frequency about the minor axis, v_0/r where $v_0 = (1/B)(\partial\Phi/\partial r)$. The physical explanation is as follows. Although the charge separation currents are stationary in the laboratory frame, relative to the plasma frame they rotate with the doppler-shifted frequency $-v_0/r$. The response of the plasma is analogous to the forced oscillation of a stationary plasma column to an externally imposed charge separation rotating at this frequency, i.e. it is inversely proportional to the dielectric constant.

The ion and electron diffusion rates in a time-invariant electric field were found to be generally unequal⁴. The condition that they be equal, which is necessary for a steady equilibrium, was satisfied only when $v_0 = 0$ i.e. zero radial space charge field. The diffusion rate then agreed with that derived by Pfirsch and Schlüter². However, this ambipolar state was found to be unstable in the sense that any departure from charge neutrality produced a difference in diffusion rates which increased the charge imbalance. The electric drift would thus be expected to increase with time until $-v_0/r$ approached the frequency of a natural mode of the plasma. The dielectric constant then tends to zero and the diffusion rate becomes very large, so large that the linearised treatment breaks down. It was proposed that a non-linear treatment would show an ambipolar state close to this resonant condition, with a diffusion rate much greater than the Pfirsch and Schlüter rate.

In this paper this analysis is extended to include the viscous force parallel to the magnetic field. Stable ambipolar states are now found for well-defined values of the radial electric field, and

the corresponding ambipolar diffusion rate is evaluated.

Section II defines the coordinate system, the simplified magnetic field used in the analysis, and the ordering assumed. Treating the zero order radial distribution of density and electrostatic potential as specified, the azimuthal variation in density and potential is derived in Sec.III. The corresponding radial diffusion rate is evaluated in Sec.IV. In a steady equilibrium in which there is no other loss process, the ion and electron diffusion rates must be equal. Equating the two diffusion rates gives a cubic equation for the ambipolar radial electric field, whose solution is discussed in Sec.V. The corresponding ambipolar diffusion rates are also evaluated. The diffusion in a time-varying electric field, and the time taken for the ambipolar field to build up, is evaluated in Sec. VI. In Sec. VII the form of the ambipolar potential distribution and the magnitude of the corresponding diffusion rates in typical experimental devices will be discussed. In Appendix A the analysis is extended to include the helical component of magnetic field in a stellarator. It is found that in most conditions of interest the effect of the helical field is small compared to the toroidal variation.

The analysis is based on guiding center fluid equations. Fluid equations are valid only so long as the mean free path is less than the connection length i.e. the distance measured along a field line as it encircles the minor axis once, $L_c = 2\pi r B/B_\theta$. For longer mean free paths the kinetic equations must be used. This condition was first considered by Galeev and Sagdeev⁵. An improved analysis, which includes the effect of azimuthal electric fields, was outlined in reference (4) and will be given in more detail in a later paper, together with a treatment for the transition between this and the

resistive regime. Since in many existing stellarators the connection length varies over the cross section from greater than to less than the mean free path, the comparison between theory and experiment will be deferred to this later paper.

II. THE MODEL

The co-ordinates and magnetic field used are the same as those discussed in reference (3). r, θ are polar co-ordinates centred on the magnetic axis, and ϕ measures angular distance along the axis as illustrated in Fig.1. Relative to these co-ordinates the magnetic field is taken to be

$$\underline{B} = \frac{R_0}{R} \left[0, B_{\theta\theta}(r), B_{\phi\phi} \right] \quad \dots (1)$$

where R_0 is the radius of the magnetic axis, $R = R_0(1 + \varepsilon \cos\theta)$, and $\varepsilon = r/R_0$. Eq.(1) is intended to represent a field of the Tokamak type, or the toroidal variation of a stellarator field. The plasma current required to produce this field flows everywhere in the ϕ direction³. The displacement of magnetic surfaces relative to the magnetic axis in a realistic toroidal field could be included by using instead of the r co-ordinate the radius of the magnetic surface passing through the point. Since this increases the analytic detail without appearing to affect the results significantly, the toroidal displacement of magnetic surfaces is neglected.

When terms of order ε are neglected, \underline{B} is azimuthally symmetric and consequently the equilibrium density and electrostatic potential must also be independent of θ . For a large aspect ratio torus all

equilibrium quantities may be expanded as a power series in ε , e.g.

$$n(r, \theta) = n_0(r) + n_1(r, \theta) + \dots, \quad \Phi(r, \theta) = \Phi_0(r) + \Phi_1(r, \theta) + \dots \quad \dots (2)$$

where $n_s(r, \theta)$ contains all terms of order $\varepsilon^s n_0$. A zero order radial temperature gradient will not be included in the following analysis.

It is hoped to include this in a later paper.

The analysis uses guiding center fluid equations. The same results can be obtained using MHD fluid equations, but then finite Larmor radius terms must be included in the parallel equation of motion, and the analysis is rather longer and less physically transparent. When guiding center equations are used the effect of finite Larmor radius corrections is generally small, and will be neglected in the following analysis. The mean guiding center velocity of a particle of the j^{th} species may be written in the form

$$\underline{v}_j = v_{\parallel} \underline{B}/|B| + \underline{v}_{bj} + \underline{v}_{cj} + \underline{v}_0 + \underline{v}_1 + \dots \quad \dots (3)$$

where

$$\underline{v}_{bj} = - \frac{2\kappa T_j}{e_j B^2 R} (B_{\phi} \underline{e}_z - B_z \underline{e}_{\phi}), \quad \underline{v}_{cj} = - \gamma_{jk} \frac{m_j \kappa T_j}{e^2 B^2 n} \nabla_{\perp} n$$

$$\underline{v}_0 = - \frac{\nabla \Phi_0 \times \underline{B}}{B^2}, \quad \underline{v}_1 = - \frac{\nabla \Phi_1 \times \underline{B}}{B^2}$$

\underline{e}_z and \underline{e}_{ϕ} are unit vectors in the vertical and ϕ directions.

\underline{v}_{bj} is the mean curvature and ∇B drift. \underline{v}_{cj} is the average guiding center collisional diffusion of the j^{th} species resulting from a density gradient across the field, where γ_{jk} is the collision frequency with the other species. This term contributes a diffusion equal to that in a straight plasma column², and for brevity it will be dropped in the following analysis.

It is convenient to express the order of magnitude of these velocities relative to the diamagnetic velocity of the j^{th} species

$$U_{jn} = \frac{\kappa T_j}{e_j B} \frac{1}{n_0} \frac{dn_0}{dr} \quad \dots (4)$$

It will be assumed that the zero order electric drift is no larger than the diamagnetic velocity, i.e. $v_0 \sim U_{jn}$, which implies

$$e \frac{d\phi_0}{dr} \sim \frac{\kappa T}{n_0} \frac{dn_0}{dr}, \quad v_1 \sim v_{bj} \sim \epsilon U_{jn} \quad \dots (5)$$

The rotational transform ι will be assumed of order unity, i.e.

$$\Theta = \frac{B_\theta}{B_\phi} = \frac{\epsilon \iota}{2\pi} = O(\epsilon).$$

If the resistivity is too large, the expansion scheme breaks down. As will be seen later from Eqs.(16) and (17), remembering that $\Theta = O(\epsilon)$, the condition for consistency is

$$\frac{\eta p'}{B^2 \Theta^2} \lesssim U_{jn} \quad \dots (6)$$

i.e. the Pfirsch and Schluter diffusion velocity must not be large compared to the diamagnetic drift velocity: when this condition is violated, the predicted diffusion rate exceeds the Bohm rate, which is thus an upper limit on the validity of the prediction.

III. EQUILIBRIUM ANALYSIS

The basic equations are the quasi-neutrality condition and the continuity equations for the ion and electron guiding center densities. Guiding center density differs from particle density by terms of order $(a_j/r)^2$, where a_j is the Larmor radius of the species⁶. Since such finite Larmor radius corrections are neglected, quasi-neutrality

implies equality of the ion and electron guiding center densities.

Rather than separately evaluating the two densities and equating the results, it is easier to satisfy quasi-neutrality by writing

$$n_e = n_i = n \quad \text{in all equations.}$$

The guiding center continuity equation is simply $\nabla \cdot (n \underline{v}_j) = 0$. As defined in Eq.(3), \underline{v}_0 has a weak azimuthal variation due to its dependence on the exact magnetic field. We first evaluate the compression due to this electric drift.

$$\nabla \cdot \underline{v}_0 = - \nabla \cdot \left(\frac{1}{B^2} \right) \cdot (\nabla \Phi_0 \times \underline{B}) + \frac{(\nabla \times \underline{B}) \cdot \nabla \Phi_0}{B^2} = - \frac{2}{R} v_{0\theta} \sin \theta \quad \dots (7)$$

Since $\nabla \times \underline{B}$ is in the ϕ direction, $(\nabla \times \underline{B}) \cdot \nabla \Phi_0 = 0$. Thus $\nabla \cdot \underline{v}_0$ is of order $\varepsilon \frac{U_{jn}}{r}$, while $\nabla \cdot \underline{v}_1$ is of order $\varepsilon^2 \frac{U_{jn}}{r}$. The magnetic drift, although constant to order ε , produces a density variation by convection of the non-uniform plasma

$$\nabla \cdot (n \underline{v}_{bj}) = - \frac{2\kappa T_j}{e_j R} \frac{B_\phi}{B^2} \frac{\partial n_0}{\partial z} = - \frac{2\kappa T_j}{e_j R} \frac{B_\phi}{B^2} \frac{dn_0}{dr} \sin \theta \quad \dots (8)$$

Retaining only first order terms in the continuity equation gives

$$(\underline{v}_0 \cdot \nabla) n_1 + (\underline{v}_1 \cdot \nabla) n_0 + n_0 \frac{\partial v_{j\parallel}}{\partial s} = \frac{2n_0}{R} \cdot \frac{B_\phi}{B} (U_{jn} + v_0) \sin \theta \quad \dots (9)$$

where

$$\frac{\partial}{\partial s} = \frac{1}{B} (\underline{B} \cdot \nabla) = \frac{B_\theta}{rB} \frac{\partial}{\partial \theta} = \frac{\Theta}{r} \frac{\partial}{\partial \theta}.$$

Since $B_\theta = O(\varepsilon B_\phi)$ is assumed, the factor $\frac{B_\phi}{B} = 1 + O(\varepsilon^2)$, and it is unnecessary to distinguish between $v_{0\theta}$ and v_0 . Subtracting Eq.(9) for the ions and electrons, and integrating with respect to θ , gives the current required to neutralise the charge separation drifts

$$j_{\parallel} = - \frac{2\varepsilon}{\Theta B} \frac{dp_0}{dr} \cos \theta. \quad \dots (10)$$

Since the mean guiding center motion parallel to the magnetic field $v_{j\parallel}$ is identical to the corresponding fluid velocity, the fluid equation of motion and the generalised Ohm's law may be used to describe this motion.

$$n m_i \frac{v_0}{r} \frac{\partial v_{i\parallel}}{\partial \theta} = - \frac{\partial p}{\partial s} + \mu_{\parallel} \frac{\partial^2 v_{i\parallel}}{\partial s^2} + \mu_{\perp} \nabla_{\perp}^2 v_{i\parallel} + \frac{\partial \mu_{\perp}}{\partial r} \left(\frac{\partial v}{\partial s} r + \frac{\partial v_{i\parallel}}{\partial r} \right) \quad \dots (11)$$

$$\eta j_{\parallel} = \frac{\Theta}{r} \frac{\partial}{\partial \theta} \left[- \Phi_1 + \frac{\kappa T_e}{n_0 e} n_1 \right] \quad \dots (12)$$

Eq.(11) differs from the usual MHD fluid equation where the inertial term on the left hand side would include the diamagnetic velocity, i.e. $n m_i (v_0 + U_{in}) \frac{\partial v_{i\parallel}}{r \partial \theta}$, while the right hand side should include the finite Larmor radius corrections to the pressure tensor^{7,8}. These corrections include the term $\frac{1}{r} \frac{\partial}{\partial r} \left(\frac{n \kappa T_i}{\Omega_i} \right) \frac{\partial v_{i\parallel}}{\partial \theta}$, which just cancels the diamagnetic inertial term. When Eq.(11) is obtained directly from the guiding center kinetic equation with collision terms, as will be done in a later paper, neither the spurious inertial term nor the compensating pressure correction arise.

The parallel and perpendicular coefficients of viscosity are given by^{7,8}

$$\mu_{\parallel} = 1.28 \frac{n \kappa T_0}{\gamma_{ii}}, \quad \mu_{\perp} = 1.2 \frac{n \kappa T_i}{\gamma_{ii}} \left(\frac{\gamma_{ii}}{\Omega_i} \right)^2 \quad \dots (13)$$

where γ_{ii} is the ion-ion collision frequency, and Ω_i the ion cyclotron frequency. The relative magnitudes of the viscous terms are

$$\left(\mu_{\perp} \nabla_{\perp}^2 v_{i\parallel} \right) / \left(\mu_{\parallel} \frac{\partial^2 v_{i\parallel}}{\partial s^2} \right) \sim \left(\frac{v_{ii}}{\Omega_i \Theta} \right)^2 \sim \left[\frac{a_i}{r} \frac{L_c}{2\pi \lambda_{mfp}} \right]^2. \quad \dots (14)$$

The most common experimental condition is $a_i \ll r$, while L_c although greater than λ_{mfp} , is not much greater. The terms resulting from the

perpendicular viscosity are then relatively small. These terms will be dropped, but they can be included by replacing ν in the following analysis by $\nu_{\parallel} + \nu_{\perp} \Theta^{-2} r^2 \nabla_{\perp}^2$. When the radial variation is neglected this is simply $\nu_{\parallel} + \nu_{\perp} / \Theta^2$. The condition where the perpendicular viscous coefficient is dominant has recently been investigated by Rosenbluth and Taylor⁹.

Substituting Eq.(10) for j_{\parallel} in Eq.(12), and integrating with respect to θ gives

$$\Phi_1 = \frac{\kappa T_e}{e} \frac{n_1}{n_0} + \frac{2\epsilon\eta r}{B\Theta^2} \frac{dp_0}{dr} \sin\theta. \quad \dots (15)$$

Before eliminating $v_{i\parallel}$ between Eq.(11) and the ion continuity equation, it is convenient to express the azimuthal variation in complex exponential form i.e. $\sin\theta$ is replaced by $-i \exp(i\theta)$ on the understanding that only the real parts of the equations have physical significance. Since the equations are linear, all the first order variables must vary as $\exp(i\theta)$. The resulting equations are then readily solved for Φ_1 and n_1 to give

$$\begin{aligned} & \left[1 + \frac{U_{en}}{v_0} - \frac{c_s^2 \Theta^2}{v_0^2} - \frac{i\nu\Theta^2}{r v_0} \left(1 + \frac{U_{en}}{v_0} \right) \right] \Phi_1 \\ &= -\frac{2\epsilon}{v_0} e^{i\theta} \left[\frac{\kappa T_e}{e} (v_0 + U_{in}) + \frac{\eta\nu p'}{B} \right] \\ & - 2i\epsilon e^{i\theta} \left[\frac{\eta p' r}{B\Theta^2} \left(1 - \frac{c_s^2 \Theta^2}{v_0^2} \right) - \frac{\kappa T_e \nu \Theta^2}{e r v_0^2} (v_0 + U_{in}) \right] \\ & \dots (16) \end{aligned}$$

$$\begin{aligned} & \left[1 + \frac{U_{en}}{v_0} - \frac{c_s^2 \Theta^2}{v_0^2} - \frac{i\nu\Theta^2}{r v_0} \left(1 + \frac{U_{en}}{v_0} \right) \right] \frac{n_1}{n_0} \\ &= -\frac{2\epsilon}{v_0} e^{i\theta} \left[v_0 + U_{in} + \frac{\eta\nu p'}{B^2 v_0} \frac{n'}{n} \right] \\ & - \frac{2i\epsilon}{v_0} e^{i\theta} \left[\frac{\eta p' r}{B^2 \Theta^2} \frac{n'}{n} - \frac{\nu \Theta^2}{r v_0} (v_0 + U_{in}) \right] \quad \dots (17) \end{aligned}$$

where $\nu = \mu_{\parallel}/n_0 m_i$ is the kinematic viscosity, c_s is the sound speed $[\kappa(T_i + T_e)/m_i]^{1/2}$, and a dash denotes differentiation with respect to r .

IV. EVALUATION OF THE DIFFUSION

The radial guiding center flux will now be integrated over a magnetic surface, $r = \text{constant}$, to obtain the net outward flux. The surface element is $dS = r d\theta R_0 (1 + \varepsilon \cos\theta) d\phi$.

$$\begin{aligned} n v_{Dj} &= - \frac{1}{2\pi r B_0} \int_0^{2\pi} (n_0 + n_1) \left[\frac{\partial \Phi}{\partial \theta} + \frac{2\varepsilon \kappa T_j}{e_j} \sin\theta \right] (1 + \varepsilon \cos\theta)^2 d\theta \\ &= - \frac{1}{2\pi r B_0} \int_0^{2\pi} \left[\frac{\partial \Phi}{\partial \theta} (2\varepsilon n_0 \cos\theta + n_1) + \frac{2\varepsilon \kappa T_j}{e_j} n_1 \sin\theta \right] d\theta \end{aligned} \quad \dots (18)$$

Although it would be hard to visualise a particle diffusion which differs from the guiding center diffusion, the fact that the local fluxes are different may raise some doubts. The identity of the two fluxes will now be demonstrated. Integrating the radial velocity, obtained from the two fluid equations of motion, over a surface gives

$$\begin{aligned} n v_{Dj} &= - \frac{1}{2\pi r B_0} \int_0^{2\pi} \left[(n_0 + n_1) \frac{\partial \Phi}{\partial \theta} + \frac{\kappa T_j}{e_j} \frac{\partial n}{\partial \theta} \right] (1 + \varepsilon \cos\theta)^2 d\theta \\ &= - \frac{1}{2\pi r B_0} \int_0^{2\pi} \left[\frac{\partial \Phi}{\partial \theta} (2\varepsilon n_0 \cos\theta + n_1) + \frac{2\varepsilon \kappa T_j}{e_j} \frac{\partial n}{\partial \theta} \cos\theta \right] d\theta \end{aligned} \quad \dots (19)$$

An integration by parts converts the last term in Eq.(19) into the last term in Eq.(18).

Before evaluating the products in Eq.(18), n_1 and Φ_1 must first be expressed in real terms. If the coefficient of Φ_1 and n_1 in

Eqs.(16) and (17) is written as $D = |D| \exp(-i\chi)$, then the real parts of the expression for Φ_1 and n_1 are of the form

$$|D| \Phi_1(r, \theta) = -N \cos(\theta + \chi) + P \sin(\theta + \chi)$$

$$|D| \frac{n_1}{n_0} = -Q \cos(\theta + \chi) + S \sin(\theta + \chi)$$

Substituting into Eq.(18) gives

$$nv_{Dj} = -\frac{\epsilon n_0}{r B_0 |D|} \left[\left(N + \frac{\kappa T_e}{e_j} Q \right) \sin \chi + \left(P + \frac{\kappa T_j}{e_j} S \right) \cos \chi + \frac{NS - PQ}{2\epsilon n_0 |D|} \right] \dots (20)$$

Substituting for N, P, Q, S and χ from Eqs.(16) and (17) gives

$$v_{Di} = -\frac{v_{ps}}{v_0^4 D^2} \left[\left(v_0^2 + v_0 U_{en} - c_s^2 \Theta^2 \right) c_s^2 \Theta^2 - \frac{c_s^2 \Theta^2 p'}{neB} (v_0 + U_{in}) J - (c_s^2 \Theta^2)^2 K/J \right] \dots (21)$$

$$v_{De} = -\frac{v_{ps}}{v_0^4 D^2} \left[\left(v_0^2 + v_0 U_{en} - c_s^2 \Theta^2 \right) \left\{ c_s^2 \Theta^2 + v_0 (U_{in} - U_{en}) \right\} + K c_s^2 \Theta^2 \left\{ (U_{in} - U_{en}) (v_0 + U_{en}) - c_s^2 \Theta^2 / J \right\} \right] \dots (22)$$

where

$$J = \frac{\nu}{\eta} \frac{p B^2 \Theta^4}{(rp')^2}, \quad K = \left(\frac{\nu \Theta}{rc_s} \right)^2$$

$$v_0^4 D^2 = \left(v_0^2 + v_0 U_{en} - c_s^2 \Theta^2 \right)^2 + K c_s^2 \Theta^2 (v_0 + U_{en})^2$$

$$v_{ps} = -\frac{2\epsilon^2 \eta p'}{B^2 \Theta^2} = \text{Pfirsch and Schlüter}^2 \text{ diffusion velocity.}$$

When $\nu = 0$ the above equations reduce to those derived in reference (4) for a purely resistive plasma. The physical origin of D is the same as in the resistive case⁴. Relative to the plasma frame the toroidal magnetic field and the resulting charge separation currents rotate at the doppler-shifted frequency $-v_0/r$. The response

of the plasma to this externally driven charge separation should be inversely proportional to the plasma dielectric constant at the appropriate frequency and wavelength. The factor D on the left hand side of Eqs.(16) and (17) agrees with the dielectric constant of a stationary resistive/viscous plasma column for an electrostatic oscillation whose frequency is $-v_o/r$, whose wavelength parallel to the magnetic field is L_c and azimuthal wave number $m = 1$. The diffusion rate is inversely proportional to D^2 .

In reference (4) the expressions for the plasma response and diffusion rates become infinite when $v_o^2 + v_o U_{en} - c_s^2 \Theta^2 = 0$. The doppler-shifted frequency then coincides with the frequency of a natural mode in the plasma, i.e. a drift/ion acoustic mode. Viscosity introduces damping, which limits the response of the plasma when driven on resonance.

V. THE AMBIPOLAR CONDITION

For a steady equilibrium the ion and electron diffusion rates must be equal. Equating Eqs.(21) and (22) gives the ambipolar condition

$$v_o(v_o^2 + v_o U_{en} - c_s^2 \Theta^2) + c_s^2 \Theta^2 \left[K(v_o + U_{en}) + J(v_o + U_{in}) \right] = 0 \quad \dots (23)$$

This relation may be used to express Eqs.(22) or (21) in a rather more convenient form for evaluation of the corresponding diffusion rate

$$v_{Da} = v_{ps} \left[1 + v_o^2 \left\{ \frac{J(v_o + U_{in})^2 + c_s^2 \Theta^2 K/J}{c_s^2 \Theta^2 M^2 + v_o^2 K(v_o + U_{en})^2} \right\} \right] \quad \dots (24)$$

where

$$M = J(v_o + U_{in}) + K(v_o + U_{en}).$$

No simple analytic solution to the cubic equation for v_0 , Eq.(23), is valid over the wide range of values of the quantities K and J of experimental interest. The parameter range will now be divided into sectors over each of which simple analytic solutions exist, and these expressions for v_0 will be substituted into Eq.(24) to give the corresponding ambipolar diffusion rate. The boundaries separating the different sectors of parameter space are shown by dashed lines in Fig.2.

The basic parameters chosen are λ_{mfp}/L_c and a_i/r_n^Θ , where r_n is the density scale length n/n' . The second parameter equals $2U_{in}/c_i^\Theta$. When viewed from the plasma rest frame the azimuthal variation in the equilibrium fields looks more like a drift wave or an ion acoustic wave, depending on whether this quantity is greater or less than unity. The quantities J and K are both proportional to $(\lambda_{mfp}/L_c)^2$.

$$K = \left(\frac{\nu_\Theta}{rc_s} \right)^2 = \left[\frac{1.28 c_i^2}{r \gamma_{ii} c_s} \right]^2 \sim \left[\frac{2\pi \lambda_{mfp}}{L_c} \right]^2 \quad \dots (25)$$

$$J = \frac{\nu_p B^2 \Theta^4}{\eta (rp')^2} \sim \frac{1.28}{1.96} \frac{c_i^2}{\gamma_{ii}} \frac{n e^2}{m \gamma_{ei}} \left(\frac{r_n}{r} \right)^2 \frac{\Theta^4 B^2}{2 n \kappa T} \sim \frac{2}{3} \left[\frac{2\pi \lambda_{mfp}}{L_c} \right]^2 \left(\frac{m_i}{m_e} \right)^{1/2} \left[\frac{r_n^\Theta}{a_i} \right]^2$$

where $a_i = (2\kappa T/m_i \Omega_i^2)^{1/2}$ is the ion Larmor radius. The ion and electron temperatures have been assumed equal to avoid introducing another parameter. For brevity the ratio $2\pi \lambda_{mfp}/L_c$ will be denoted by λ .

Case (a) $(a_i/r_n^\Theta) > (m_i/m_e)^{1/4}$

In this range the term proportional to J may be neglected in Eq.(23). The three solutions for the ambipolar electric drift v_0 , which are sketched in Fig.3a, are approximately

$$(i) \text{ when } \lambda < r_n^\Theta/a_i, v_0 \approx -U_{en} - c_s^2 \Theta^2 / U_{en}, \quad c_s^2 \Theta^2 / U_{en}, \quad K U_{en}$$

(ii) when $\lambda > r_n^\ominus/a_i$, $v_o \approx -U_{en}$, two solutions imaginary.

The corresponding values of the ambipolar diffusion rate are respectively

$$(i) \quad \frac{v_{Da}}{v_{ps}} \approx \frac{c_s^2 \Theta^2}{J(v_o + U_{en})^2} \sim \frac{3}{8\lambda^2} \left(\frac{m_e}{m_i}\right)^{\frac{1}{2}} \left(\frac{a_i}{r_n^\ominus}\right)^4 \quad \dots (26)$$

$$\frac{v_{Da}}{v_{ps}} \approx \frac{c_s^2 \Theta^2}{J(v_o + U_{en})^2} \sim \frac{6}{\lambda^2} \left(\frac{m_e}{m_i}\right)^{\frac{1}{2}} \quad \dots (27)$$

$$\frac{v_{Da}}{v_{ps}} \approx \frac{K}{J} \sim 1.2 \left(\frac{m_e}{m_i}\right)^{\frac{1}{2}} \left(\frac{a_i}{r_n^\ominus}\right)^2. \quad \dots (28)$$

$$(ii) \quad \frac{v_{Da}}{v_{ps}} \approx \left(\frac{U_{en}}{c_s^\ominus}\right)^2 \frac{1}{J} \sim \frac{3}{8\lambda^2} \left(\frac{m_e}{m_i}\right)^{\frac{1}{2}} \left(\frac{a_i}{r_n^\ominus}\right)^4. \quad \dots (29)$$

All the above rates are higher than Pfirsch and Schlüter, the solution corresponding to $v_o = -U_{en}$ giving the most rapid diffusion.

Case (b) $1 < a_i/r_n^\ominus < (m_i/m_e)^{\frac{1}{4}}$

In this range the term proportional to K may be neglected in Eq.(23). The three solutions, illustrated in Fig.3b, are approximately

$$(i) \quad \lambda < \left(\frac{m_e}{m_i}\right)^{\frac{1}{4}}, v_o \approx -U_{en} - \frac{c_s^2 \Theta^2}{U_{en}}, \frac{c_s^2 \Theta^2}{U_{en}}, JU_{in}$$

$$(ii) \quad \text{when} \quad \left(\frac{m_e}{m_i}\right)^{\frac{1}{4}} < \lambda < \left(\frac{m_e}{m_i}\right)^{\frac{1}{4}} \left(\frac{a_i}{r_n^\ominus}\right)^2, v_o \approx -U_{en}, \pm c_s^\ominus J^{\frac{1}{2}}$$

$$(iii) \quad \text{when} \quad \lambda > \left(\frac{m_e}{m_i}\right)^{\frac{1}{4}} \left(\frac{a_i}{r_n^\ominus}\right)^2, v_o \approx -U_{in}, \text{ two roots imaginary.}$$

The corresponding values of the ambipolar diffusion rate are respectively

$$(i) \quad \frac{v_{Da}}{v_{ps}} \sim \frac{c_s^2 \Theta^2}{J(v_o + U_{en})} \sim \frac{3}{8\lambda^2} \left(\frac{m_e}{m_i}\right)^{\frac{1}{2}} \left(\frac{a_i}{r_{n\Theta}}\right)^4 \quad \dots (30)$$

$$\frac{v_{Da}}{v_{ps}} \approx \left(\frac{v_o}{c_s \Theta}\right)^2 \frac{1}{J} \sim \frac{3}{\lambda^2} \left(\frac{m_e}{m_i}\right)^{\frac{1}{2}}, \quad \text{and} \quad \frac{v_{Da}}{v_{ps}} \approx 1 \quad \dots (31)$$

(ii)

$$\frac{v_{Da}}{v_{ps}} \approx \left(\frac{U_{en}}{c_s \Theta}\right)^2 \frac{1}{J} \sim \frac{3}{8\lambda^2} \left(\frac{m_e}{m_i}\right)^{\frac{1}{2}} \left(\frac{a_i}{r_{n\Theta}}\right)^4 \quad \dots (32)$$

$$\frac{v_{Da}}{v_{ps}} \approx 2 \quad \text{for the other two roots.} \quad \dots (33)$$

(iii)

$$v_{Da} \approx v_{ps}.$$

In ranges (b) (i) and (b) (ii) the $v_o \approx -U_{en}$ solution again gives the fastest diffusion.

Case (c) $a_i/r_{n\Theta} < 1$

The solutions of Eq.(23), illustrated on Fig.3c, are approximately

(i) when

$$\lambda < \left(\frac{m_e}{m_i}\right)^{\frac{1}{4}} \frac{a_i}{r_{n\Theta}}, \quad v_o \approx \pm c_s \Theta, \quad JU_{in}$$

(ii) when

$$\lambda > \left(\frac{m_e}{m_i}\right)^{\frac{1}{4}} \frac{a_i}{r_{n\Theta}}, \quad v_o \approx -U_{in} (1 + 1/J),$$

and two imaginary roots.

The corresponding ambipolar diffusion rates are

$$\frac{v_{Da}}{v_{ps}} \sim \frac{1}{J} \sim \frac{3}{2} \left(\frac{m_e}{m_i}\right)^{\frac{1}{2}} \left(\frac{a_i}{\lambda r_{n\Theta}}\right)^2 \quad \text{for } v_o = \pm c_s \Theta \quad \dots (34)$$

$$v_{Da} \approx v_{ps} \quad \text{for } v_o = JU_{in}.$$

(ii)

$$v_{Da} \approx v_{ps}$$

In view of the number of terms in the expressions for the ambipolar potential and diffusion rate, it is not surprising that there are no simple approximations which are universally valid. The most consistent root is $v_0 \approx -U_{en}$, which satisfies the ambipolar condition in regions a(i), a(ii), b(i) and b(ii). The corresponding diffusion velocity is given by Eq.(26) throughout. This can exceed the Pfirsch and Schlüter diffusion by several orders of magnitude.

VI. BUILD-UP TIME FOR THE AMBIPOLAR POTENTIAL DISTRIBUTION

In a practical confinement system the initial radial variation in potential, determined by plasma injection or formation processes, will not generally coincide with one of the ambipolar distributions found in the previous Section. The subsequent build-up of the electric field towards an ambipolar distribution will now be considered.

The time variation in the electric field will introduce a new term into Eq.(3) for the guiding center velocity i.e. the inertial correction

$$\underline{v}_{tj} = \frac{1}{\Omega_j B} \frac{d\underline{E}}{dt} = -\frac{1}{\Omega_j} \frac{\partial v_0}{\partial t} \underline{e}_r - \frac{1}{\Omega_j B} \frac{d}{dt} \left(\underline{v}_1 \times \underline{B} \right) \quad \dots (35)$$

where $\Omega_j = e_j B / m_j$ and \underline{e}_r is a unit vector in the radial direction. The rate of change in v_0 should certainly be slow compared to the ion cyclotron frequency, i.e. $\partial v_0 / \partial t \lesssim 0 (\epsilon \Omega_i v_0)$, in which case v_{tj} does not contribute any first order terms to the linearised equations for the azimuthal variations.

The rate of change of n_1 and $v_{i||}$ with time should be included

in the continuity equations and the parallel component of the fluid equation of motion, respectively. However, if the rate of change is assumed slow, i.e. $\frac{\partial}{\partial t} < 0 \left(\frac{\epsilon v_o}{r} \right)$, these terms do not enter any of the first order equations of Sec. III.

Since the radial flux vanishes to first order when integrated over a magnetic surface, the contribution of the inertial correction to the net flux can be significant. Eq.(18) is modified to

$$\begin{aligned} n v_{dj} &= - \frac{1}{2\pi r B_o} \int_0^{2\pi} (n_o + n_1) \left[\frac{\partial \Phi_1}{\partial \theta} + \frac{2\epsilon \kappa T_j}{e_j} \sin \theta + \frac{r B}{\Omega_j} \frac{\partial v_o}{\partial t} \right] (1 + \epsilon \cos \theta)^2 d\theta \\ &= n_o v_{Dj} - \frac{n_o}{\Omega_j} \frac{\partial v_o}{\partial t}, \end{aligned} \quad \dots (36)$$

where v_{Dj} is the diffusion velocity calculated on the assumption of a steady electric field, as given by Eq.(21) and (22). This still gives the net flux due to the $\underline{E} \times \underline{B}$ and magnetic drifts, since n_1 and Φ_1 , are unaffected by the time variation.

Quasi-neutrality requires that $v_{di} = v_{de}$ at all times. Hence

$$\begin{aligned} \frac{\partial v_o}{\partial t} &= \Omega_1 (v_{Di} - v_{De}) \\ &= \frac{v_{ps} c_s^2}{v_o^4 D^2} \frac{1}{i_o} \frac{dn_o}{dr} \left[v_o \left(v_o^2 + v_o U_{en} - c_s^2 \Theta^2 \right) \right. \\ &\quad \left. + c_s^2 \Theta^2 \left\{ K(v_o + U_{en}) + J(v_o + U_{in}) \right\} \right]. \end{aligned} \quad \dots (37)$$

The corresponding equation in reference (9) differs from the above in that $v_{||}$ is replaced by v_{\perp}/Θ^2 in the definition of J , since only the perpendicular coefficient of viscosity was included, and terms proportional to v^2 are omitted in D^2 and in the numerator.

As may be seen from Fig.3, where there are three ambipolar electric fields, one is always positive, one is negative, while the middle one can be of either sign. From the sign of $v_{De} - v_{Di}$ shown in Fig.4, it may be seen that this middle solution is always unstable in the sense that, if v_o is initially close to this ambipolar value, it will steadily move further away from it. The outer two ambipolar fields are always stable. Thus v_o will move towards that stable ambipolar value which lies on the same side of the unstable solution as the initial v_o . When only one ambipolar electric field exists, this is always stable, and the radial electric field will approach this value irrespective of its initial value.

An order of magnitude estimate will now be made of the time taken for v_o to approach the diamagnetic drift velocity, assuming it does not first reach an ambipolar value. Normalising $v_{Di} - v_{De}$ to the Pfirsch and Schlüter velocity gives

$$\tau_E = \frac{U_{en}}{\partial v_o / \partial t} = \frac{M}{m} \frac{1}{\gamma_{ei}} \left(\frac{l}{2\pi} \right)^2 \left(\frac{\tau}{1+\tau} \right) \frac{v_{ps}}{(v_{Di} - v_{De})} \dots (38)$$

The variation of $v_{De} - v_{Di}$ with v_o is sketched in Fig.4 for one particular range of plasma parameters, such that there is only one ambipolar field, denoted by v_{oa} . Over most of the range of v_o , $v_{De} - v_{Di} \sim 2v_{ps}$. Taking this as typical, the build-up time given by Eq.(38) is generally appreciably less than the experimental duration.

A rough check will now be made on the consistency of Eq.(37) with the original assumption of slow variation on the equilibrium distribution. Expressed in terms of the parameters plotted in Fig.2

$$\frac{r}{v_o^2} \frac{\partial v_o}{\partial t} \sim \left(\frac{m}{M} \right)^{1/2} \left(\frac{L_c}{2\pi\lambda_{mfp}} \right) \left(\frac{r_{n^0}}{a_i} \right) \left(\frac{2\pi}{l} \right)^2 \left(\frac{U_{en}}{v_o} \right)^2 \frac{(v_{Di} - v_{De})}{v_{ps}} \dots (39)$$

Typically $L_c/2\pi\lambda_{mfp} \sim 3$, $r_n^\ominus/a_i \sim 0.1$, $v_{Di} - v_{De} \sim 2v_{ps}$. Hence this ratio is less than ε provided v_o/U_{en} and ι are not too small.

The inertial correction to the ion diffusion adjusts itself so that the ion and electron rates are equal. Since the effect of time variation on the electron diffusion is negligible, the common rate during the build-up phase is given by Eq.(22). In the typical condition illustrated in Fig.4, this is comparable to the Pfirsch and Schlüter rate over most of the range of v_o .

VII. A TYPICAL AMBIPOLAR POTENTIAL DISTRIBUTION

The solid lines in Fig.2 show the variation in the parameters over the cross-section for one typical operating condition in each of a number of toroidal experiments¹⁰ (where an experiment can operate in a number of significantly different modes, a line is shown for parameters typical of each mode). The density scale length r_n has been arbitrarily taken as one-fifth of the plasma radius. The variation over the cross section is large for $\ell = 3$ stellarators, due to the variation in rotational transform. The value of the parameters at half the plasma radius is marked by a cross.

The upper limit on $2\pi\lambda_{mfp}/L_c$ for validity of the fluid results will be considered in a later paper. They should be valid up to the value unity, and perhaps some distance beyond. Except for L1 and T3, the experiments lie at least partly within the range of validity of the fluid theory.

As an example, the case where the plasma is in condition a(ii) near the axis, passes through condition b(ii) as radius and rotational transform increases, and reaches condition c(ii) near the

edge, will be considered. Model C and PROTO-CLEO stellarators both follow this pattern in some operating conditions. The variation of the ambipolar electric field with radius is illustrated in Fig.5. There is only one solution to the ambipolar condition in regions a(ii) and c(ii), given by $v_o \approx -U_{en}$ and $v_o \approx -U_{in}$ respectively. In region b(ii) there are three solutions, the middle one of which is unstable. At some radius the electric field must flip over from the upper to the lower stable curves, giving a sharp reversal of the radial electric field. ABDEF and ABCEF are two possible stable ambipolar field distributions. In practice the flip-over point will depend on the initial potential distribution. The ambipolar diffusion rate along section CDEF is comparable to the Pfirsch and Schlüter rate, while along ABC it can be much greater. Thus the overall diffusion rate will depend on where the flip-over occurs.

VIII. CONCLUSIONS

It has been shown that, when inertia and parallel viscosity are included in the equilibrium equations, radial electric fields inevitably build up in a toroidal resistive plasma in order to equalise the ion and electron diffusion rates. The time to reach the ambipolar potential distribution is found to be less than the duration of a typical experiment.

There is no simple general expression for the corresponding ambipolar diffusion rate, but simple expressions have been obtained for the different regions in parameter space. This ambipolar diffusion may be much more rapid than the earlier prediction by Pfirsch and Schlüter². This is because the ambipolar electric field usually lies

close to the resonant field. This is the electric field at which the rotating plasma sees the toroidal variation at a doppler-shifted frequency equal to the frequency of a natural plasma wave, e.g. an electron-drift wave.

The measured diffusion rates in most toroidal experiments are significantly greater than the equilibrium diffusion predicted by earlier theories. In some cases it is as much as three orders of magnitude greater¹⁰. Most of these experiments lie at least partly in the intermediate collision frequency range where fluid equations are not applicable. This range will be considered in a later paper. By combining the predictions for the two regimes it is hoped to come closer to explaining the observed diffusion.

ACKNOWLEDGEMENT

I am indebted to J.D. Jukes for drawing my attention to the importance of parallel viscosity in the equilibrium equations.

REFERENCES

1. M.D. Kruskal and R.M. Kulsrud, Phys. Fluids 1, 265 (1958).
2. D. Pfirsch and A. Schlüter, Max-Planck Institut, Report No. MPI/PA/7/62 (1962) (unpublished).
3. G. Knorr, Phys. Fluids 8, 1334 (1965).
4. T.E. Stringer, Phys. Rev. Letters 22, 770 (1969).
5. A.A. Galeev and R.Z. Sagdeev, ZETF 53, 348 (1967); Sov. Phys.-JETP, 26, 233 (1968).
6. G. Schmidt, "Physics of High Temperature Plasmas" (Academic Press, New York, 1966), p.292.
7. S.I. Braginskii, in "Reviews of Plasma Physics" (Consultants Bureau, New York, 1965), Vol.1, p.205.
8. W.B. Thompson, "Introduction to Plasma Physics" (Pergamon Press, London, 1962), p.228.
9. M.N. Rosenbluth and J.B. Taylor, Phys. Rev. Letters 23, 367 (1969).
10. R.J. Bickerton and A. Gibson in Culham report CLM-L 18 (unpublished), (1968).

APPENDIX

THE EFFECT OF A HELICAL FIELD

The equilibrium analysis given in Sec. III will now be extended to include the helical field component in a toroidal stellarator. The field of a toroidal stellarator will be approximated to by the magnetic potential

$$\psi = B_0 R_0 \left[\varphi + \frac{\delta}{\alpha} I_\ell(\ell a r/R) \sin \ell(\theta - \alpha \varphi) \right] \quad \dots (A1)$$

$$\underline{B} = \nabla \psi = \left[\frac{\partial}{\partial r}, \frac{1}{r} \frac{\partial}{\partial \theta}, \frac{1}{R_0(1+\varepsilon \cos \theta)} \frac{\partial}{\partial \varphi} \right] \psi \quad \dots (A2)$$

δ and ε will be assumed to be small quantities of the same order. Since only first order terms are required, all equations can be linearised in δ and ε

e.g.

$$B \approx B_\varphi \approx B_0 \left[1 - \varepsilon \cos \theta - \ell \delta I_\ell(\ell a r/R) \cos \ell(\theta - \alpha \varphi) \right] \quad \dots (A3)$$

$$\Phi(r, \theta, \varphi) = \Phi_0(r) + \Phi_1^{(\varepsilon)}(r, \theta) + \Phi_1^{(\delta)}(r, \theta - \alpha \varphi), \text{ etc.}$$

The guiding center drift is now the sum of toroidal and helical components. Its radial component, which enters the continuity equation, is

$$v_{bjr} = - \frac{2\kappa T_j}{e_j r B} \left[\varepsilon \sin \theta + \ell^2 \delta I_\ell(\ell a r/R) \sin \ell(\theta - \alpha \varphi) \right] \quad \dots (A4)$$

The change in $\Phi_1^{(\varepsilon)}$ along a field line is small over one helical field period. Consequently we may average $\partial/\partial s$ over the helical field period giving

$$\frac{\partial \Phi^{(\varepsilon)}}{\partial s} = \frac{\Theta}{r} \frac{\partial \Phi^{(\varepsilon)}}{\partial \theta} \quad \dots (A5)$$

as in Sec.III. The scale length for variation of $\Phi_1^{(\delta)}$ along a field line is the helical field period. Over one such period the mean rotation of a field line is small, and can be neglected. Hence,

$$\frac{\partial \Phi_1^{(\delta)}}{\partial s} = \frac{1}{R} \frac{\partial \Phi_1^{(\delta)}}{\partial \varphi} . \quad \dots (A6)$$

Rotational transform can easily be included in this derivative, but merely replaces some α factors by $(\alpha - t/2\pi)$.

The analogue of Eq.(10) for $j_{||}$ now includes a term proportional to $\delta \cos \ell(\theta - \alpha\varphi)$, this being the current required to neutralise the charge separation drifts in the helical field variation. Because of their different θ dependence, terms which are functions of θ and those which are functions of $\theta - \alpha\varphi$ must separately vanish. The resulting expressions for $\Phi_1^{(\varepsilon)}$ and $n_1^{(\varepsilon)}$ are identical to Eqs.(16) and (17). The corresponding expressions for $\Phi_1^{(\delta)}$ and $n_1^{(\delta)}$ may be obtained from Eqs.(16) and (17) by the following substitutions

$$\varepsilon \rightarrow \delta \ell^2 I_\ell(\ell \alpha r/R), \quad \Theta \rightarrow -\varepsilon \alpha, \quad \theta \rightarrow \ell(\theta - \alpha\varphi). \quad \dots (A7)$$

When the radial flux is integrated over a magnetic surface, as in Eq.(18), only products of terms having the same θ variation survive. The diffusion is now the sum of toroidal and helical components. The toroidal component is still given by Eqs.(21) and (22). The helical component may be obtained from Eqs.(21) and (22) by making the substitutions given in Eq.(A7). The factor corresponding to v_{ps} in these equations is

$$(v_{ps})_h = -2 \frac{\left[\delta \ell^2 I_\ell(\ell \alpha r/R) \right]^2}{B^2 \varepsilon^2 \alpha^2} \eta p' \quad \dots (A8)$$

This factor is more readily evaluable for specific experiments when δ is expressed in terms of the rotational transform ι produced by the helical field. Assuming $\ell\alpha r/R < 1$,

$$\frac{\iota}{2\pi} \approx \left[\delta \ell I_\ell(\ell\alpha r/R) \right]^2 (\ell-1)/\ell\alpha^3 \varepsilon^4 \quad \dots (A9)$$

$$(v_{ps})_h \approx - \frac{2\varepsilon^2 \eta p'}{B^2} \left(\frac{\iota}{2\pi} \right) \frac{\alpha \ell^3}{(\ell-1)} \cdot \quad \dots (A10)$$

The ratio of this to the corresponding factor for the toroidal component is

$$\frac{(v_{ps})_h}{(v_{ps})_t} = \varepsilon^2 \left(\frac{\iota}{2\pi} \right)^3 \frac{\alpha \ell^3}{(\ell-1)} \cdot \quad \dots (A11)$$

Here $\alpha = 2\pi R/L_w$, where L_w is the helical winding period. This ratio is $\lesssim 0(10^{-1})$ in all experimental conditions of interest. For an $\ell=3$ stellarator it varies as r^8 , and so is very small over most of the cross section. The terms multiplying v_{ps} will generally be comparable for the helical and toroidal diffusion rates. Thus (A11) gives an order of magnitude estimate of the two diffusion rates.

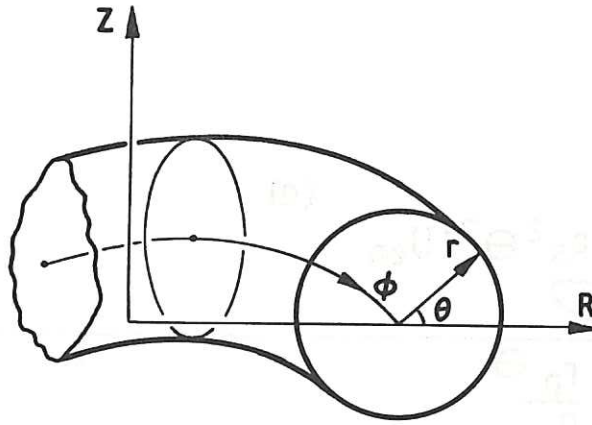


Fig.1 The co-ordinates.

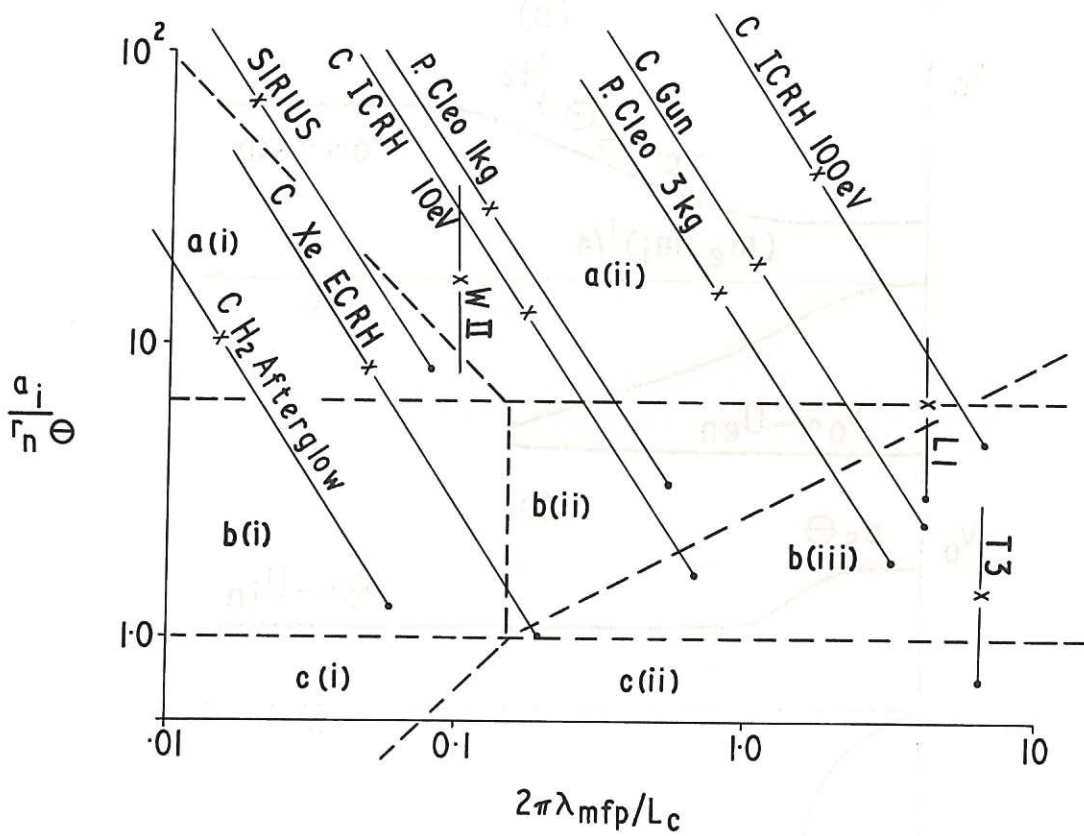


Fig.2 Regions of validity of approximations for the ambipolar diffusion condition (dashed lines) and typical experimental parameters (solid lines).

- L1 = Lebedev L1 stellarator with gun plasma
- WII = Garching Wendelstein II Barium stellarator
- C = Princeton Model C stellarator
- P.CLEO = Culham PROTO-CLEO stellarator
- Sirius = Kharkov Sirius stellarator
- T3 = Kurchatov T3 Tokamak

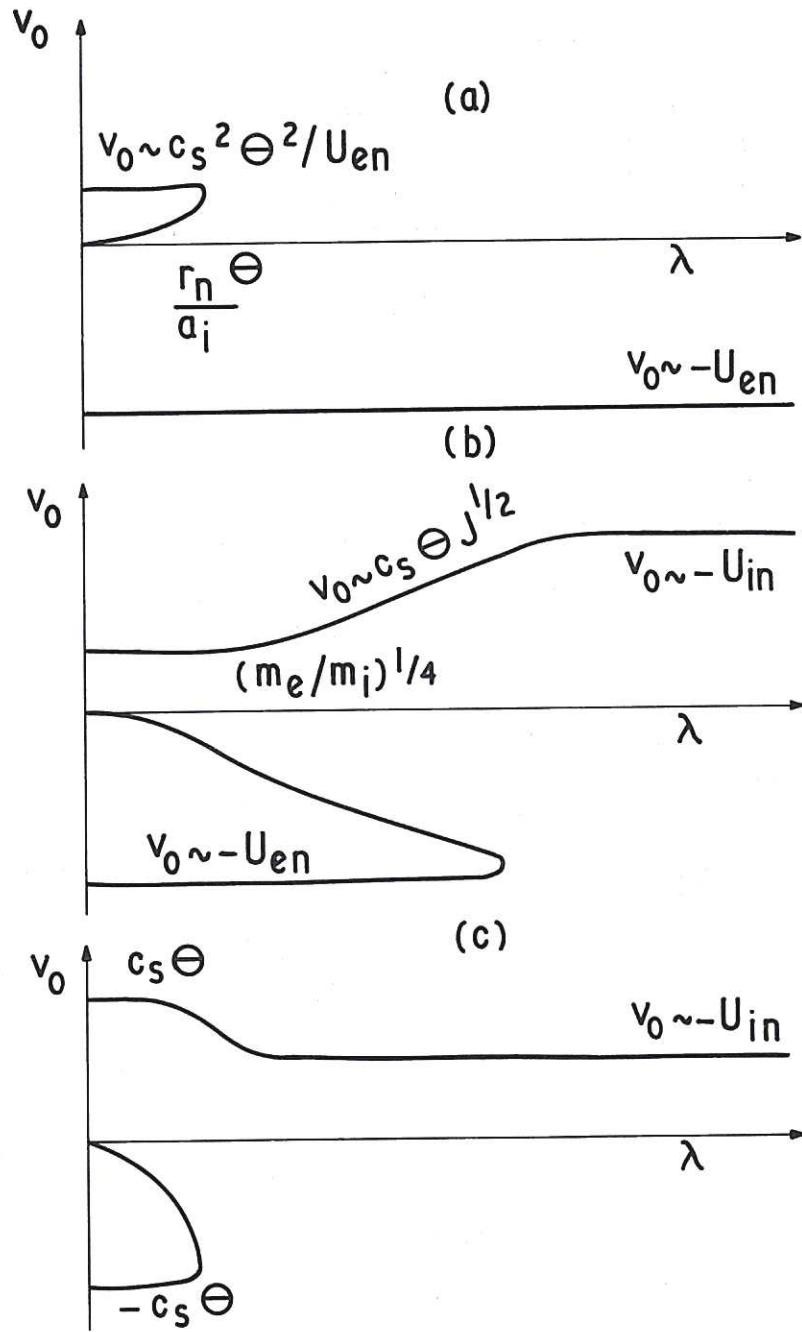


Fig.3 Variation of the ambipolar electric drifts with mean free path.

$$(a) \quad \frac{a_i}{r_n \Theta} > \left(\frac{m_i}{m_e} \right)^{1/4}, \quad (b) \quad 1 < \frac{a_i}{r_n \Theta} < \left(\frac{m_i}{m_e} \right)^{1/4}$$

$$(c) \quad \frac{a_i}{r_n \Theta} < 1.$$

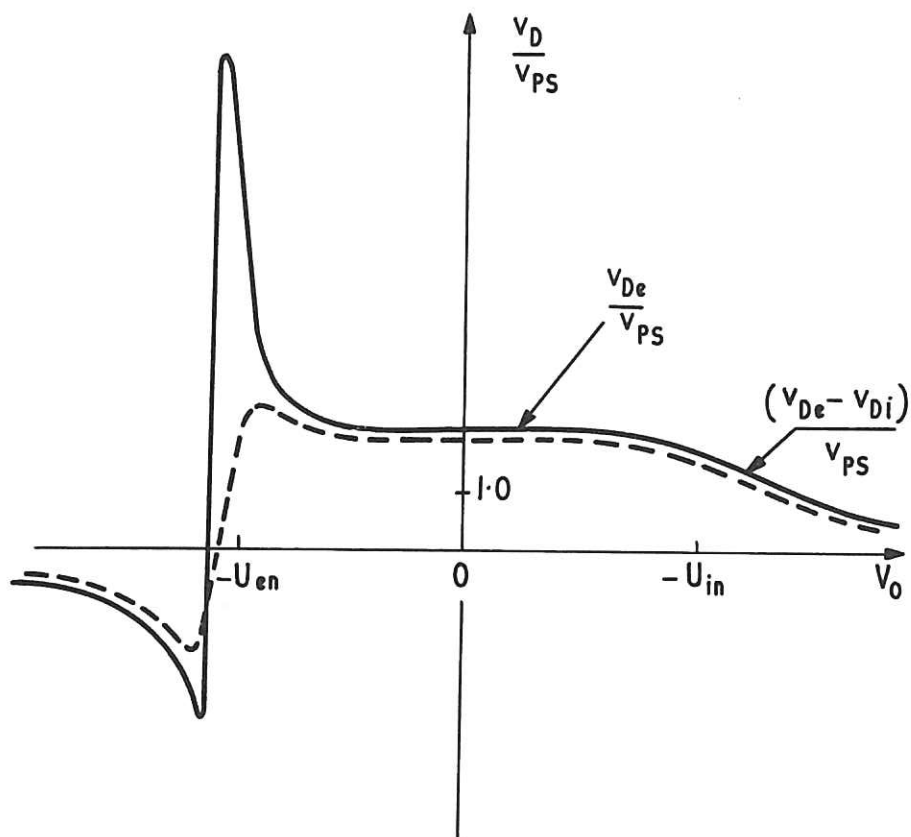


Fig.4 Dependence of the diffusion velocities on the electric rotation velocity

$$\frac{a_i}{r_n \Theta} > \left(\frac{m_i}{m_e} \right)^{1/4}, \quad \frac{2\pi\lambda_{mfP}}{L_c} > \left(\frac{m_e}{m_i} \right)^{1/4}.$$

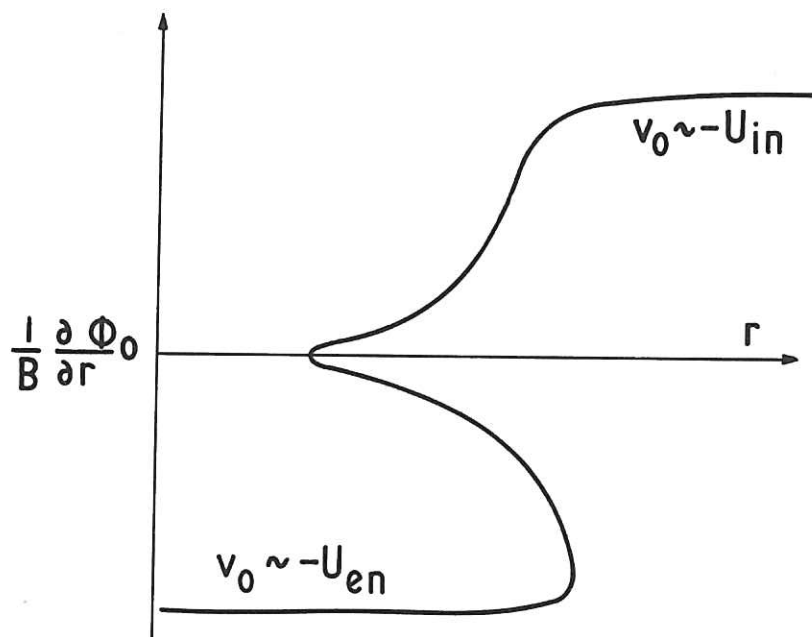


Fig.5 A typical variation of the ambipolar electric field with radius.

